β-Sheet Structures and Dimer Models of the Two Major Tyrocidines, Antimicrobial Peptides from Bacillus aneurinolyticus

ARTICLE *in* BIOCHEMISTRY · OCTOBER 2013

Impact Factor: 3.02 · DOI: 10.1021/bi401363m · Source: PubMed

BIOCHEMISTRY
including biophysical chemistry & molecular biology

Article

pubs.acs.org/biochemistry

β-Sheet Structures and Dimer Models of the Two Major Tyrocidines, Antimicrobial Peptides from *Bacillus aneurinolyticus*

Gadzikano Munyuki,[†,‡] Graham E. Jackson,[†] Gerhard A. Venter,[†] Katalin E. Kövér,[§] László Szilágyi,[§] Marina Rautenbach,[∥] Barbara M. Spathelf,[∥] Bhaswati Bhattacharya,[∥] and David van der Spoel*[,‡]

[†]Department of Chemistry, University of Cape Town, P Bag X3, Rondebosch, Cape Town, South Africa 7701

[‡]Uppsala Center for Computational Chemistry, Science for Life Laboratory, Department of Cell and Molecular Biology, Uppsala University, Husargatan 3, Box 596, SE-751 24 Uppsala, Sweden

[§]Department of Chemistry, University of Debrecen, H-4010 Debrecen, Egyetem tér 1, Pf. 20, Hungary

[∥]BIOPEP Peptide group, Department of Biochemistry, Stellenbosch University, Stellenbosch, South Africa 7600

Supporting Information

ABSTRACT: The structures of two major tyrocidines, antibiotic peptides from *Bacillus aneurinolyticus*, in an aqueous environment were studied using nuclear magnetic resonance spectroscopy, restrained molecular dynamics (MD), circular dichroism, and mass spectrometry. TrcA and TrcC formed β-structures in an aqueous environment. Hydrophobic and hydrophilic residues were not totally separated into nonpolar and polar faces of the peptides, indicating that tyrocidines have low amphipathicity. In all the β-structures, residues Trp^4/Phe^4 and Orn^9 were on the same face. The ability of the peptides to form dimers in aqueous environment was studied by replica exchange MD simulations. Both peptides readily dimerize, and predominant complex structures were characterized through cluster analysis. The peptides formed dimers by either associating sideways or stacking on top of each other. Dimers formed through sideways association were mainly stabilized by hydrogen bonding, while the other dimers were stabilized by hydrophobic interactions. The ability of tyrocidine peptides to form different types of dimers with different orientations suggests that they can form larger aggregates, as well.

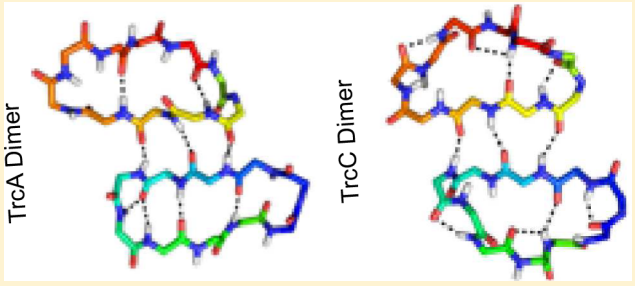

The discovery of tyrothricin, a mixture of antimicrobial peptides consisting of the linear gramicidins and cyclic decapeptides, denoted the tyrocidines, in the late 1930s is credited to Rene Dubos.[1−3] A wide variety of tyrocidines have been isolated from tyrothricin.[4,5] Tyrocidine A (TrcA), tyrocidine B (TrcB), and tyrocidine C (TrcC) are the most abundant and together with the minor tyrocidines make up 60% of the tyrothricin complex produced by *Bacillus aneurinolyticus*.[5] They have a highly conserved cyclo(D-Phe^1-L-Pro^2-L-X^3-D-X^4-L-Asn^5-L-Gln^6-L-Tyr^7-L-Val^8-L-Orn^9-L-Leu^{10})[6] sequence involving both D and L amino acids. The sequences differ at residues L-X^3-D-X^4 (L-Phe^3-D-Phe^4, L-Trp^3-D-Phe^4, and L-Trp^3-D-Trp^4 in TrcA, TrcB, and TrcC, respectively). Despite their excellent ability to kill bacteria such as the food-borne pathogen *Listeria monocytogenes*,[7] which causes listeriosis, the use of tyrocidine peptides is currently limited to topical applications[1] because they are also hemolytic, leading to erythrocyte lysis. As with most antimicrobial peptides, the tyrocidines are membrane active and the bactericidal activity is due to the disruption of the membrane structure through either lysis or the formation of pores, resulting in cell death. Despite their hemolytic activity, the tyrocidines have a broad spectrum of activity, including antifungal activity,[8] and are highly selective toward the erythrocytic stages of the malaria parasite, *Plasmodium falciparum*.[9] However, the antiplasmodium activity is not dependent on lytic activity, and the tyrocidines may have an alternative intraparasitic target, indicating that they also can enter cells. Similarly, the tyrocidine may also have alternative targets in bacteria.[10,11] The tyrocidines are potential candidates as new therapeutic agents against a number of pathogens because of their broad spectrum of activity, their rapid membranolytic mechanism of action, and the possibility of alternative targets limiting resistance potential.

The activity of antimicrobial peptides is determined by their three-dimensional structures and physicochemical properties. Studies involving gramicidin S, a cyclic decapeptide with a sequence 50% identical with those of the tyrocidines, sharing the conserved pentapeptide unit (D-Phe-Pro-Val-Orn-Leu), have shown that physicochemical properties such as size, amphipathicity, hydrophobicity, conformation, and charge distribution play crucial roles in regulating activity.[12−14] Similarly, it has been shown that the tyrocidine structure−activity relationships toward different target cells are dependent

Received: October 3, 2013
Published: October 8, 2013

   dx.doi.org/10.1021/bi401363m | *Biochemistry* 2013, 52, 7798−7806

on different physicochemical properties. In particular, antiplasmodium activity was correlated with a small size and hydrophobicity,[9] while antibacterial activity was correlated with higher polarity.[7] Some of these physicochemical properties such as charge distribution and amphipathicity are determined by the three-dimensional structure of the peptide. Self-assembly, another important property that influences the mechanism of action of antimicrobial peptides, depends on a number of these factors such as hydrophobicity, amphipathicity, conformation, and the general topology of the peptide.[12−16]

Small, linear, and cyclic peptides are known to aggregate and/or self-assemble in different ways in different environments, and this influences their activities as antimicrobial peptides. Tyrocidines have been shown to aggregate in solution,[17−20] but the molecular interaction driving tyrocidine aggregation and/or self-assembly in water is not fully understood. Gramicidin S is known to self-assemble when it interacts with a phospholipid membrane, forming a channel structure that disrupts the cell membrane potential,[21,22] resulting in cell death. Smaller cyclic D- and L-β-peptides have been extensively studied, as well. They typically form planar conformations and self-assemble by stacking, resulting in hollow channels in which all the side chains in the peptides lie on the outside of the channel.[23−26] Protegrin, a β-sheet disulfide-bonded cyclic peptide, also assembles by sideways overlap as it disrupts membrane lipid packing.[27] Studies have shown that self-association and multimerization are crucial for peptide activity.[28] β-Structures have been shown to disrupt the cell membrane potential,[21,22] resulting in cell death. β-Sheet peptides, such as the tyrocidines, are likely to undergo superstructure organization upon membrane interaction,[28] and such multimer formation has been suggested to play a key role in the cytolytic activity of β-sheet peptides.[15,16,29,30] However, self-assembly in aqueous solution is expected to impact membrane interaction and reduce antibacterial activity.[30−33] It is, therefore, important to understand the role of self-assembly in the mechanism of action of tyrocidines.

In this study, we aim to elucidate the dimeric structures, as the seeding structure of self-assembly and membrane activity of tyrocidines in water. TrcA is the most hydrophobic and most active peptide against *P. falciparum*,[9] while the more polar TrcC showed the most activity against bacteria[7] and fungi.[8] Nuclear magnetic resonance (NMR) spectroscopy, restrained molecular dynamics, circular dichroism (CD), and electrospray ionization mass spectrometry were used to study the two different tyrocidines and to determine their solution structure. Replica exchange molecular dynamics simulations of TrcA and TrcC dimers were used to investigate the energy landscape for dimerization.

METHODS

NMR Experiments. The tyrocidine samples were prepared from commercial tyrothricin (Sigma-Aldrich) as described by Rautenbach et al.[9] The peptides (1−2 mg) were dissolved in 0.5 mL of a 10:1 (v/v) H_2O/D_2O solution. The solution was adjusted to pH 4 by adding a few drops of DCl. Trimethylsilylpropionate (TSP) was used as the internal chemical shift reference.

^{1}H NMR experiments were performed on Bruker Avance 400 MHz and Avance II 500 MHz spectrometers. Coupling constants were measured from the one-dimensional ^{1}H NMR spectra. The two-dimensional NMR spectra of the peptide in water were recorded in the phase sensitive mode, TOCSY (mixing time, 60 ms),[34] NOESY (mixing time, 100 ms),[35] and ROESY (mixing time, 150 ms),[36] using the WATERGATE sequence to suppress the water resonance.[37] Spectral assignments were based on the method of Wüthrich.[38] Interproton distances, from the two-dimensional (2D) nuclear Overhauser effect (NOE) cross-peak intensities, were estimated by the isolated spin pair approximation (ISPA):[39]

$$r_{ij} = r_{\mathrm{ref}}(a_{\mathrm{ref}}/a_{ij})^{1/6}$$

where r_{ij} is the interproton distance to be estimated and a_{ij} is the corresponding 2D NOE cross-peak intensity.

Simulated Annealing Conformational Search. The starting configurations of the peptides were generated using homology modeling. The structure of gramicidin S was used as the template. An initial conformational search was performed using molecular dynamics in vacuum at 600 K for 100 ns using the GROMACS molecular dynamics package.[40] The OPLS force field was used in the calculations.[41] A time step of 2 fs was used, and the nonbonded interactions were treated with a cutoff function operating at 1.2 nm. Structures were saved every 1 ns, and all the saved structures were subjected to simulated annealing for 1 ns. The structure that had the lowest energy after annealing was subjected to molecular dynamics in water for 100 ns.

Restrained Molecular Dynamics in Water. NMR-derived distance restraints (Tables S5 and S6 of the Supporting Information) were applied with a force constant of 1000 kJ mol^{-1} nm^{-2}. The peptide starting conformation was placed in a box with dimensions of 3.3 nm × 3.6 nm × 4.1 nm. The box was solvated with water using the Simple Point Charge (SPC) model.[42] Energy minimization using the steepest descent algorithm was performed to remove high-energy contacts in the systems. The systems were equilibrated by a short simulation of 1 ns. Protein and solvent were coupled separately to an external bath using a time constant of 0.1 ps according to the Berendsen method.[43] The systems were also coupled to an external pressure bath using a time constant of 0.1 ps and a reference pressure of 1 bar based on the Berendsen method. Lennard-Jones and Coulombic nonbonded interactions were treated with a cutoff and PME[44] operating at 1.2 and 1.0 nm, respectively. All the covalent bonds were constrained using the LINCS algorithm.[45] The neighbor list was updated after every 10 steps, and a time step of 2 fs was used.

Circular Dichroism Experiments. Analytical stock solutions (2.00 mg/mL) of the purified tyrocidines were prepared in ethanol/water mixtures [1:1 (v/v)] and diluted to 10 μM in water. CD scans were obtained on a Chirascan CD spectrometer (Applied Photophysics) using a 1.00 cm quartz cuvette. Three scans were collected between 190 and 250 nm with 0.1 nm steps. The spectra of the blank solutions were autosubtracted.

Dimerization Simulations. The first step in the aggregation process, dimerization, was studied for both tyrocidines. Replica exchange molecular dynamics (REMD) simulations[46,47] were used to study the dimerization process of TrcA and TrcC peptides under constant-pressure (1 bar) conditions. REMD allows a system to perform a random walk in the potential energy surface such that it escapes local minimum states, in which it could otherwise have been trapped.[48] REMD is also employed to accelerate sampling. Twenty-six unrestrained replicas with temperatures ranging from 300 to 400 K were used for the REMD simulations of

dx.doi.org/10.1021/bi401363m | *Biochemistry* 2013, 52, 7798−7806

both systems. The temperatures were generated using the temperature generator for REMD simulations[49] based on an exchange probability of 0.2. The simulations were run for 100 ns for each replica with an exchange tried every 10 ps and storing data every 20 ps. The other simulation parameters were identical to those for monomer simulations.

Electrospray Mass Spectrometry. Purified tyrocidines were analyzed via high-resolution time-of-flight electrospray mass spectrometry (TOF-ESMS). Direct injection TOF-ESMS analysis of the two purified tyrocidines at 200 μg/mL in an acetonitrile/water mixture [1:1 (v/v)] was performed on a Waters Synapt G2 TOF mass spectrometer fitted with an electrospray ionization source. The peptides were subjected to a capillary voltage of 3.0 kV with a source voltage of 15 V and a source temperature of 120 °C. Data were collected in the positive continuum mode by scanning over an m/z range of 300−2000. Multiprotonated spectra were deconvoluted using the MaxEnt 3 algorithm of Mass Lynx version 4.1, with a calculated range from 300 to 6500 amu, a maximum of 10 charges, 50 iterations, and auto-peak width determination.

RESULTS

Molecular Structures of Tyrocidines. *NMR.* The NMR assignments and chemical shifts of the two peptides are listed in Tables S1 and S2 of the Supporting Information. Correlations between proton chemical shifts and the secondary structure of peptides and proteins identified in earlier studies[50−52] were utilized to obtain more structural information about the two tyrocidines. Helical Hα and HN protons have chemical shifts that are consistently smaller than their respective random coil values by ∼0.3 ppm, while for β-sheets, the opposite is true.[50,51,53] However, the involvement of amide protons in hydrogen bonding affects their chemical shifts, thereby limiting their use as a qualitative indicator of structure.[54] Aromatic ring currents[55] and sequence effects[56] can also affect the ^{1}H chemical shifts, complicating the interpretation of the spectra of these tyrocidines that have four aromatic residues in their decapeptide structure.

Figure S1 of the Supporting Information shows the Hα and HN random coil chemical shift deviations ($\Delta\delta$) of the two tyrocidines in water. All of the HN and Hα chemical shifts of TrcA were larger than their random coil values by >0.3 ppm except for the HN chemical shifts of Phe3, which had a $\Delta\delta$ of −0.113 ppm. Similarly, TrcC had two residues with an amide proton $\Delta\delta$ of <0.3 ppm. These were −0.31 and −0.02 ppm for Trp^3 and Val^8, respectively. It was also observed that TrcC had only three residues with Hα $\Delta\delta$ values of <0.3 ppm (Phe^1, Pro^2, and Trp^3). These results suggest β-sheet structures for these two peptides. The HN random coil chemical shift deviations of Phe^3/Trp^3 can be attributed to the ring current effects of neighboring aromatic Phe^4/Trp^4 residues, but they could also be due to its involvement in hydrogen bonding in the peptides.

$^3J_{HNH\alpha}$ coupling constants can be useful for structure determination if they assume values of <5 or >8 Hz,[57] because between 5 and 8 Hz the $^3J_{HNH\alpha}$ coupling constants can correspond to four dihedral angles.[38] A $^3J_{HNH\alpha}$ coupling constant of <5 Hz is indicative of an α-helical conformation, whereas a $^3J_{HNH\alpha}$ of >8 Hz shows the presence of a β-sheet structure.[58] The MD simulation results were used to calculate the $^3J_{HNH\alpha}$ coupling constants of the tyrocidine peptides[59] in water and compare them to those determined from NMR (Table 1). The Karplus equation[60] was used to calculate the $^3J_{HNH\alpha}$ coupling constants for the MD simulations with parameters due to Vuister and Bax.[61] $^3J_{HNH\alpha}$ coupling constants from NMR were very similar for the two peptides and agree well with the MD $^3J_{HNH\alpha}$ coupling constants. The $^3J_{HNH}$ coupling constants point to the presence of β-sheets in the peptides. The temperature coefficients of TrcA were measured, and the results were consistent with the hydrogen bonding network that was observed during MD.

Table 1. NMR and MD ^{1}H−^{1}H Coupling Constants (hertz) of Tyrocidines

	NMR $^3J_{HNH\alpha}$ coupling constant		MD $^3J_{HNH\alpha}$ coupling constant	
residue	TrcA	TrcC	TrcA	TrcC
Phe^1	4.0	1.7	5.7	5.4
Pro^2	–	–	–	–
Trp^3/Phe^3	8.8	8.6	7.6	8.7
Trp^4/Phe^4	9.8	9.5	7.2	8.4
Asn^5	7.5	7.9	9.2	8.5
Gln^6	4.0	2.6	4.9	6.0
Tyr^7	9.9	9.7	9.2	8.6
Val^8	9.0	9.0	8.8	8.9
Orn^9	9.5	8.6	9.1	7.7
Leu^{10}	9.2	9.0	8.9	9.5

NMR Restrained Molecular Dynamics in Water. To visualize the NOE patterns, an NOE matrix for each of the tyrocidine peptides was constructed (Tables S3 and S4 of the Supporting Information). Off-diagonal elements on the matrices indicate long-range NOEs. TrcA had eight long-range NOEs and TrcC had 16. Table 2 shows the sum of violations in the restrained MD simulations, the average violation, and the number of NOE-derived distance restraints that were used to calculate the structures of the tyrocidines. The simulations for TrcA achieve somewhat better correspondence with the data than those for TrcC.

Table 2. Distance Restraint Data for TrcA and TrcC, Linearly Averaged over 100 ns of Restrained Simulation

	TrcA	TrcC
sum of violations	0.198 nm	0.650 nm
no. of restraints	32	32
average violation	0.005 nm	0.011 nm

The presence of hydrogen bonds in the peptides during restrained MD of tyrocidine monomers and unrestrained REMD of tyrocidine dimers is given in Table 3. More backbone−backbone intramolecular hydrogen bonds were found in the TrcA and TrcC peptides during restrained monomer MD simulations than in the unrestrained REMD dimer simulations (which are described below).

Representative structures from TrcA and TrcC monomer simulations are shown in Figure 1. The analysis of conformers indicated that there was no distinctive separation of hydrophilic and hydrophobic residues, indicating no overt amphipathic nature to the monomers. The representative structure of TrcA showed two strong backbone−backbone Phe^3 O−NH Leu^{10} and Asn^5 NH−O Val^8 hydrogen bonds. In earlier reports,[62,63] two additional backbone−backbone hydrogen bonds (Phe^3 NH−O Leu^{10} and Asn^5 O−NH Val^8) were found and were consistent with what was observed during the simulation (Table 3). The structure obtained showed β-sheet conformations between residues Trp^3−Asn^5 and Val^8−Leu^{10}.

dx.doi.org/10.1021/bi401363m | Biochemistry 2013, 52, 7798−7806

Table 3. Presence of Backbone Intramolecular Hydrogen Bonds for the Peptides during Monomer and Dimer Simulations as the Percentage of the Total Simulation Time[a]

	monomers		dimers			
hydrogen bond	TrcA	TrcC	TrcA monomer 1	TrcA monomer 2	TrcC monomer 1	TrcC monomer 2
Phe^1 O–NH Trp^3/Phe^3	1	5	2	2	61	60
Asn^5 O–NH Tyr^7	0	45	19	18	3	3
Gln^6 O–NH Val^8	0	0	1	1	40	43
Trp^3/Phe^3 NH–O Leu^{10}	40	29	47	54	0	0
Trp^3/Phe^3 O–NH Leu^{10}	99	97	16	10	63	63
Asn^5 NH–O Val^8	94	99	60	59	3	3
Asn^5 O–NH Val^8	16	92	21	1	3	3
total	2.5	3.7	1.7	1.5	1.7	1.8

[a] Trp^3/Phe^3 represents the Trp^3 residue for TrcC and Phe^3 for TrcA. The total indicates number of intramolecular backbone hydrogen bonds on average.

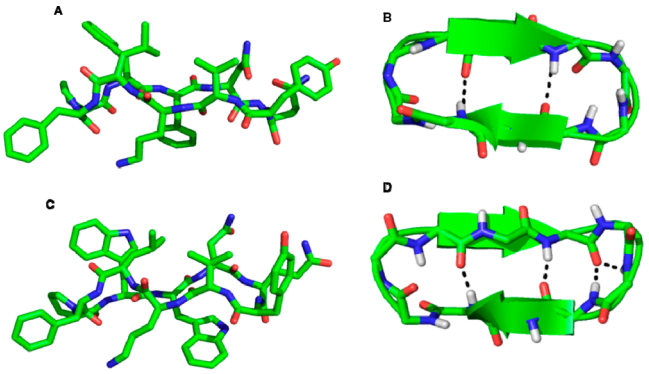

Figure 1. Representative conformations (A and C) and secondary structures (B and D) of TrcA and TrcC, respectively, in water. Hydrogen bonds are shown as dashed lines.

The representative structure of TrcC showed continuous and important intramolecular hydrogen bonds. The structure had Trp^3 O–NH Leu^{10}, Asn^5 O–HN Val^8, and Val^8 O–HN Asn^5 hydrogen bonds in water. These findings suggest that, in aqueous solution, TrcC forms antiparallel β-sheet elements between residues Trp^3–Asn^5 and Val^8–Leu^{10} as shown in panels C and D of Figure 1. Being cyclic peptides, TrcA and TrcC contained two turns each, a type II′ turn and a type I turn (Table 4).

The secondary structures of tyrocidine peptides in aqueous solution were further analyzed by Ramachandran plots (Figure 2). These plots indicated that residues of TrcA and TrcC reside in three different regions, the β-region, the α-region, and the type II or disallowed region. Six residues, Phe^3, Phe^4, Asn^5, Val^8, Orn^9, and Leu^{10}, were found in the β-region. Three residues, Pro^2, Gln^6, and Tyr^7, were located in the α-region, whereas only one residue, Phe^1, was found in the disallowed region of the Ramachandran plot (Figure 2). Glycine or residues that constitute turn regions in peptides are often found in this region,[64] but D-amino acids in both type II′ and type I′ turns can also be found here.[65] Residues that were not found in the

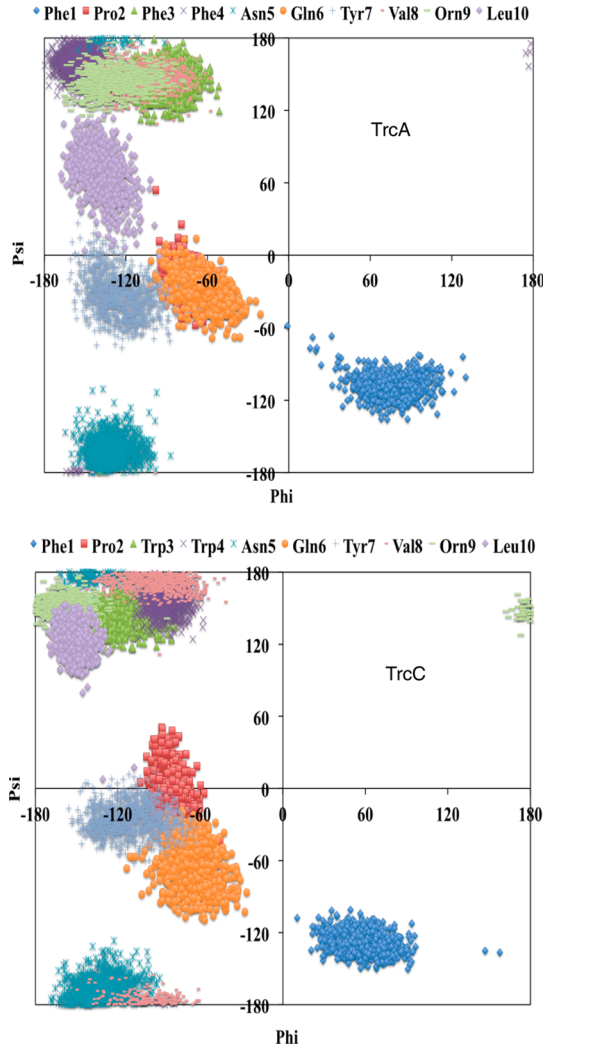

Figure 2. Ramachandran plots of the backbone dihedral angles of tyrocidines in water.

Table 4. Characterization of the Turn Regions in TrcA and TrcC Peptides Based on Restrained MD Simulations

peptide	turn	type	$i+1$	$i+2$	φ_{i+1} (deg)	ψ_{i+1} (deg)	φ_{i+2} (deg)	ψ_{i+2} (deg)
TrcA	1	II′	Phe^1	Pro^2	74 ± 15	−108 ± 9	−77 ± 7	−20 ± 11
	2	I	Gln^6	Tyr^7	−65 ± 13	−27 ± 12	−124 ± 16	−33 ± 17
TrcC	1	II′	Phe^1	Pro^2	82 ± 14	−125 ± 8	−81 ± 7	1 ± 14
	2	I	Gln6	Tyr^7	−65 ± 12	−61 ± 18	−109 ± 19	−26 ± 12

dx.doi.org/10.1021/bi401363m | *Biochemistry* 2013, 52, 7798–7806

β-region of the Ramachandran plots were part of the turn regions of the peptide.

Correlations between Tyrocidine Self-Assembly and Antimicrobial Activity. A CD-derived parameter, the negative ellipticity minima ratio in water ($\theta_{205}/\theta_{216,water}$), was chosen as an indicator of conformation and self-assembly in an aqueous environment (Figure 3). Although the obtained CD

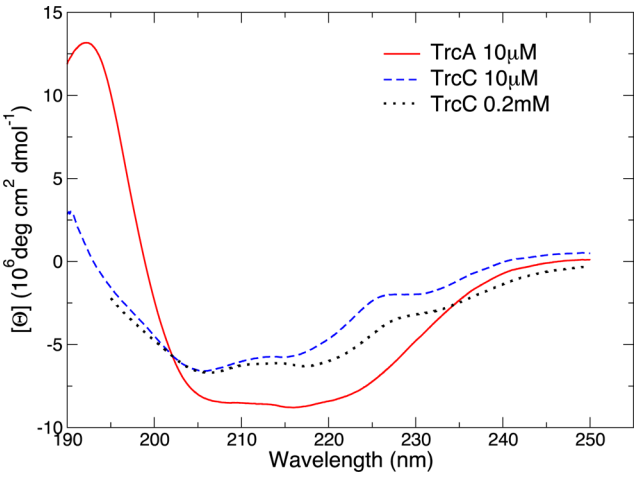

Figure 3. CD spectra of the two tyrocidines in solution. Spectra are the average of multiple determinations. For TrcC, two different concentrations were measured.

spectra of the tyrocidines (Figure 3) indicate an α-helical structural component, previous research on small cyclic peptides concluded that these negative ellipticities are due to type II′ β-turn (205−207 nm) and β-sheet (215−225 nm) structures.[13,66−69] The shape and intensity of the minima are influenced by the aromatic amino acids as well as the aggregation and/or self-assembly state of the peptide.[69] The CD spectra of TrcA and TrcC in water exhibited negative ellipticity minima at 206 and 217 nm, with $\theta_{205}/\theta_{217}$ ratios of 0.958 and 1.221, respectively. A change in this ratio indicates a backbone change, a change in hydrogen bonding pattern, and/or a change in the contribution of the aromatic amino acid residues.[69] TrcC had a maximum at 224 nm that is due to D-Trp[4]. The more hydrophobic peptide, TrcA, however, showed more intense negative ellipticities at both minima, as well as a positive ellipticity at 192 nm. These results indicate the existence of β-sheet structures, in both TrcA and TrcC (Figure 3), which is in good agreement with the NMR results. TrcC at a 20-fold higher concentration exhibited an increase in the 217 nm ellipticity and $\theta_{205}/\theta_{217}$ ratio of 1.026, similar to that of TrcA, indicating a concentration-dependent β-sheet assembly.

Dimerization of Tyrocidines in Water. *Mass Spectrometry.* Both tyrocidines formed highly stable dimers and trimers under ESMS conditions (Figure 4), with the TrcA dimers being the dominant species observed contrary to the TrcC monomer being the dominant species. Tetramers and pentamers of TrcA were also observed, which correlated with the CD results showing that TrcA has more hydrogen-bonded structures. This result also corresponded with the decrease in the level of HPLC retention (or hydrophobicity) of TrcC and indicated that the more hydrophobic TrcA has a more pronounced tendency to form dimeric and higher-order structures.

REMD Simulations. The distance between the centers of mass of the peptide pairs and the angle between the planes of

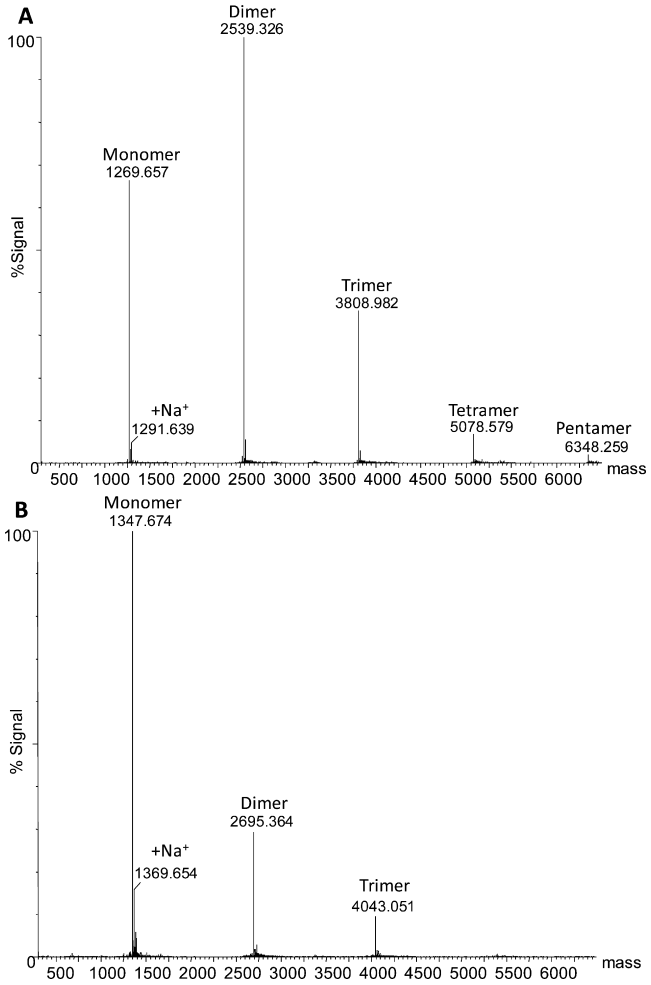

Figure 4. ESMS-TOF-transformed mass spectra for the two purified tyrocidines: (A) TrcA and (B) TrcC. The mass spectra the oligomeric species of each of the purified peptides are shown: (A) TrcA monomer (expected M_r = 1269.655), TrcA dimer (expected M_r = 2539.309), TrcA trimer (expected M_r = 3808.964), TrcA tetramer (expected M_r = 5078.619), and TrcA pentamer (expected M_r = 6348.273) and (B) TrcC monomer (expected M_r = 1347.676), TrcC dimer (expected M_r = 2695.353), and TrcC trimer (expected M_r = 4043.029).

the two peptides were monitored in the REMD simulation trajectories. The results shown (Figure 5) are based on the replicas at 300 K. Dimer conformations were assigned to different clusters using the method described by Daura et al.[70] Backbone atoms (N, Cα, and C) of the whole dimer structure were used to determine the root-mean-square-difference (rmsd). Structures were regarded as similar if their rmsd was $\leq$0.3 nm. The structure with the largest number of neighbors and all its neighbors were regarded as a cluster and eliminated from the pool of structures. The process was repeated until all the structures were put in their respective clusters. The relative population of the clusters can be derived from the simulations (Figure 5). The first five clusters of TrcA and TrcC consisted of 44 and 53% of all the saved structures, respectively. Note, however, that the absolute population of dimers and higher-order aggregates depends on peptide concentration. Most of the clusters shown contain at least one backbone−backbone hydrogen bond between the peptides. However, a good number of dimers did not have backbone−backbone hydrogen bonds. It was noted that some dimers are stabilized by π-

dx.doi.org/10.1021/bi401363m | *Biochemistry* 2013, 52, 7798−7806

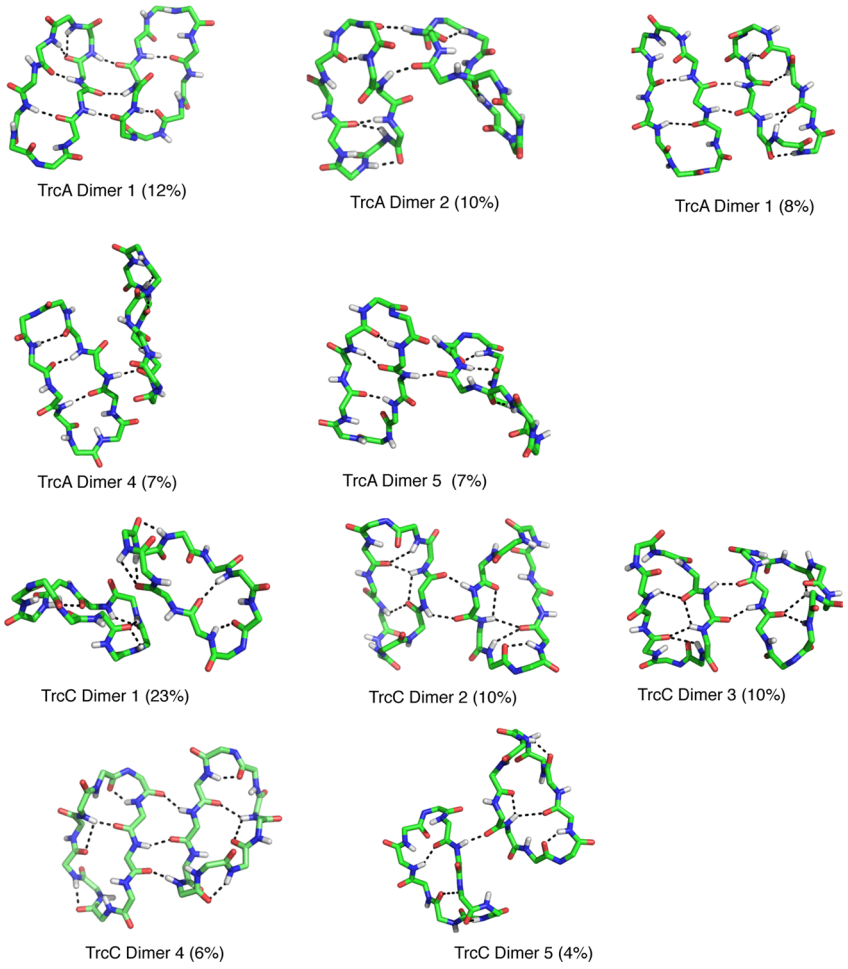

Figure 5. Representative structures for the top five most populated clusters of TrcA and TrcC along with the fractions of time the clusters were populated in the simulation at 300 K.

stacking interactions between aromatics rings of the aromatic residues in the peptides. The dissociation constants (K_d) of TrcA and TrcC dimers were determined from the fraction of time in the simulations at 300 K that the peptides were bound to be 6.7 and 10 μM, respectively, indicating that TrcA has a slightly higher binding affinity. The structures found in the most prominent dimers are quite different from the monomeric structures of the respective peptides.

DISCUSSION

Tyrocidines have a sequence 50% identical to that of gramicidin S.[71] According to our NMR, CD, and modeling studies, the tyrocidines form antiparallel β-sheets in solution, reminiscent of the well-known β-sheet structure of gramicidin S in solution.[72−74] The main difference between the tyrocidines and gramicidin S structures is the distribution of polar and nonpolar side chains around the peptides. Gramicidin S shows a total separation of hydrophilic and hydrophobic residues making it very amphipathic.[75] Conversely, there is no overt separation of hydrophobic and hydrophilic residues between the faces of the tyrocidines, indicating that they have minimal amphipathicity in monomeric form. The distribution of residues around tyrocidines is similar to that of protegrins, another class of β-sheet-forming peptides that are cyclized by two disulfide bonds. The dimerization process of tyrocidine indicated that it does form different types of dimers (Figure 5). The dimers in which peptides form backbone−backbone hydrogen bonds by sideways overlap lead to an amphipathic structure with the hydrophobic residues separated from the polar residues. In this dimeric conformation and, possibly, in longer oligomers, the cationic residues could interact with negative phospholipid headgroups of a membrane, with the D-Trp^4/D-Phe^4 residues interacting with the acyl groups, thereby anchoring the dimer. The hydrophobic cluster could then also integrate into the membrane because of the hydrophobic effect, while the polar residues interact with the phospholipid headgroups. The stable dimer structures that we observed under modeling conditions may be the seeding active structures that will allow the tyrocidines to interact with their membrane targets.

The ability of tyrocidines to form different types of dimers with different orientations suggests that they might be able to form larger aggregates or even porelike structures. Monomers could be added on both ends of the dimers, resulting in long oligomers that could traverse the membrane. Tyrocidine could therefore potentially assemble in double-helical pores similar to those proposed for the analogous gramicidin S.[76] It has been hypothesized that gramicidin S pores could be very stable inside the membrane, resulting in a loss of membrane potential that can cause cell death.[76] There is also a possibility that the tyrocidines could form oligomers that are similar to those of the amyloid β-protein (Aβ), which has recently been shown to have

dx.doi.org/10.1021/bi401363m | *Biochemistry* 2013, 52, 7798−7806

antimicrobial properties.[77] A study of protegrins 1 has indicated that it can form fibrils that are similar to those formed by Aβ and antimicrobial peptides that are rich in β-sheets.[77] The resultant fibrils have been hypothesized to form channels that can destroy the membrane structure.[78] The similarity between all these peptides suggests the possibility that peptides that are rich in β-sheets can form similar structures.[77]

■ ASSOCIATED CONTENT

Supporting Information

Additional tables containing chemical shift and NOE assignments, NOE matrices, and NOE-derived distance restraints as well as a figure showing deviations from random coil shifts. This material is available free of charge via the Internet at http://pubs.acs.org.

■ AUTHOR INFORMATION

Corresponding Author

*Telephone: +46184714205. E-mail: david.vanderspoel@icm.uu.se.

Funding

K.E.K. and L.Sz. are grateful for Grants TÁMOP-4.2.2.A-11/1/KONV-2012-0025 and OTKA K 105459. The Swedish National Infrastructure for Computing is acknowledged for a grant to D.v.d.S. (SNIC-025/12-15) and the Swedish Research Links for a collaboration grant between G.E.J. and D.S. (VR-2009-6502). EDP and NRF are acknowledged for funding to G.M.

Notes

The authors declare no competing financial interest.

■ REFERENCES

(1) Van Epps, H. L. (2006) René Dubos: Unearthing antibiotics. *J. Exp. Med. 203*, 259.
(2) Dubos, J. R. (1939) Studies on a bactericidal agent extracted from a soil bacillus. *J. Exp. Med. 70*, 1−10.
(3) Dubos, R. (1939) Studies on a bactericidal agent extracted from a soil bacillus. *J. Exp. Med. 70*, 11−17.
(4) Hotchkiss, R. D. (1940) Bactericidal fractions from an aerobic sporulating bacillus. *J. Biol. Chem. 136*, 803−804.
(5) Tang, X. J., Thibault, P., and Boyd, R. K. (1992) Characterization of the tyrocidine and gramicidin fractions of the tyrothricin complex from *Bacillus brevis* using liquid chromatography and mass spectroscopy. *Int. J. Mass Spectrom. Ion Processes 122*, 153−179.
(6) Dubos, R. J., and Hotchkiss, R. D. (1941) The production of bactericidal substances by aerobic sporulating bacilli. *J. Exp. Med. 73*, 629−640.
(7) Spathelf, B. M. (2009) Anti-listerial activity and structure−activity relationships of the six major tyrocidines, cyclic decapeptides from *Bacillus aneurinolyticus*. *Bioorg. Med. Chem. 17*, 5541−5548.
(8) Vosloo, J. A., Stander, M. A., Leussa, A. N.-N., Spathelf, B. M., and Rautenbach, M. (2013) Manipulation of the tyrothricin production profile of *Bacillus aneurinolyticus*. *Microbiology*, DOI: 10.1099/mic.0.068734-0.
(9) Rautenbach, M., Volk, N. M., Stander, M., and Hoppe, H. C. (2007) Inhibition of malaria parasite blood stages by tyrocidines, membrane-active cyclic peptide antibiotics from *Bacillus brevis*. *Biochim. Biophys. Acta 1768*, 1488−1497.
(10) Dubos, R. J., Hotchkiss, D. R., and Coburn, A. F. (1942) The effect of gramicidin and tyrocidine on bacterial metabolism. *J. Biol. Chem. 146*, 421−426.
(11) Danders, W., Marahiel, M. A., Krause, M., Kosui, N., Kato, T., Izumiya, N., and Kleinkauf, H. (1982) Antibacterial action of gramicidin S and tyrocidines in relation to active transport, *in vitro* transcription, and spore outgrowth. *Antimicrob. Agents Chemother. 22*, 785−790.
(12) Kondejewski, L. H., Jelokhani-Niaraki, M., Farmer, S. W., Lix, B., Kay, C. M., Sykes, B. D., Hancock, R. E. W., and Hodges, R. S. (1999) Dissocialtion of antimicrobial and hemolytic activities in cyclic peptide diastereomers by systematic alterations in amphipathicity. *J. Biol. Chem. 274*, 13181−13192.
(13) Kondejewski, L. H., Farmer, S. W., Wishart, D. S., Kay, C. M., Hancock, R. E. W., and Hodges, R. S. (1996) Modulation of structure and antibacterial and hemolytic activity by ring size in cyclic gramicidin S analogs. *J. Biol. Chem. 271*, 25261−25268.
(14) Kondejewski, L. H., Lee, D. L., Jelokhani-Niaraki, M., Farmer, S. W., Hancock, R. E. W., and Hodges, R. S. (2002) Optimization of microbial specificity in cyclic peptides by modulation of hydrophobicity within a defined structural framework. *J. Biol. Chem. 277*, 67−74.
(15) Hwang, P. M., and Vogel, H. J. (1998) Structure-function relationships of antimicrobial peptides. *Cell Biol. 76*, 235−246.
(16) Frecer, V., Ho, B., and Ding, J. (2004) *De novo* design of potent antimicrobial peptides. *Antimicrob. Agents Chemother. 48*, 3349−3357.
(17) Ruttenberg, M. A., King, T. P., and Craig, L. (1966) The chemistry of tyrocidine. VII. Studies on association behavior and implications regarding conformation. *Biochemistry 5*, 2857−2863.
(18) Ruttenberg, M. A., King, T. P., and Craig, L. C. (1965) The use of the tyrocidines for the study of conformation and aggregation behavior. *J. Am. Chem. Soc. 87*, 4196−4198.
(19) Parente, E., Giglio, M. A., Ricciardi, A., and Clementi, F. (1998) The combined effect of nisin, leucocin F10, pH, NaCl and EDTA on the survival of *Listeria monocytogenes* in broth. *Int. J. Food Microbiol. 40*, 65−75.
(20) Laiken, S. L., Printz, M. P., and Craig, L. C. (1971) Studies on the mode of self-assembly of tyrocidine B. *Biochem. Biophys. Res. Commun. 43*, 595−600.
(21) Hancock, R. E. W., and Chapple, D. S. (1999) Peptide Antibiotics. *Antimicrob. Agents Chemother. 43*, 1317−1323.
(22) Giuliani, A., Pirri, G., and Nicoletto, S. F. (2007) Antimicrobial peptides: An overview of a promising class of therapeutics. *Cent. Eur. J. Biol. 2*, 1−33.
(23) Bong, D. T., Clark, T. D., Granja, J. R., and Ghadiri, M. R. (2001) Self-assembling organic nanotubes. *Angew. Chem., Int. Ed. 40*, 988−1011.
(24) Ghadiri, M. R., Granja, J. R., Milligan, R. A., McRee, D. E., and Khazanovich, N. (1993) Self-assembling organic nanotubes based on a cyclic peptide architecture. *Nature 366*, 324−327.
(25) Khuran, E., Nielsen, S. O., Ensing, B., and Klein, M. L. (2006) Self-Assembling Cyclic Peptides: Molecular Dynamics Studies of Dimers in Polar and Nonpolar Solvents. *J. Phys. Chem. B 110*, 18965−18972.
(26) Tarek, M., Maigret, B., and Chipot, C. (2003) Molecular Dynamics Investigation of an Oriented Cyclic Peptide Nanotube in DMPC Bilayers. *Biophys. J. 85*, 2287−2298.
(27) Bolintineanu, D. S., and Kaznessis, Y. N. (2011) Computational studies of protegrin antimicrobial peptides: A review. *Peptides 32*, 188−201.
(28) Yount, N., and Yeaman, M. R. (2005) Immunocontinuum; perspectives in antimicrobial peptide mechanisms of action and resistance. *Protein Pept. Lett. 12*, 49−67.
(29) Glukhov, E., Stark, M., Burrows, L. L., and Deber, C. M. (2005) Basis for selectivity of cationic antimicrobial peptides for bacterial versus mammalian membranes. *J. Biol. Chem. 280*, 33967−33967.
(30) Scolani, A., Dalla Serra, M., Amodeo, P., Mannina, L., Vitale, R. M., Segre, A. L., Cruciani, O., and Menestrina, G. (2004) Structure, conformation and biological activity of a novel lipodepsipeptide from *Pseudomonas corrugata*: Cormycin A. *Biochem. J. 384*, 25−36.
(31) Rydlo, T., Rotem, S., and Mor, A. (2006) Antibacterial properties of dermaseptin S4 derivatives under extreme incubation conditions. *Antimicrob. Agents Chemother. 50*, 490−497.
(32) Shai, Y. (2002) Mode of action of membrane active antimicrobial peptides. *Biopolymers 66*, 236−248.

(33) Bechinger, B., and Lohner, K. (2006) Detergent-like actions of linear amphipathic cationic antimicrobial peptides. *Biochim. Biophys. Acta 1758*, 1529−1539.
(34) Braunschweiler, L., and Ernst, R. R. (1983) Coherence transfer by isotropic mixing: Application to proton correlation spectroscopy. *J. Magn. Reson. 53*, 521−528.
(35) Jeener, J., Meier, B. H., Bachmann, R., and Ernst, R. R. (1979) Investigation of exchange processes by two-dimensional NMR spectroscopy. *J. Chem. Phys. 71*, 4546−4553.
(36) Bax, A., and Davis, D. G. (1985) Practical aspects of two-dimensional transverse NOE spectroscopy. *J. Magn. Reson. 63*, 207−213.
(37) Sklenar, V., Piotto, M., Leppik, R., and Saudek, V. (1993) Gradient-tailored water suppression for $^{1}H—^{15}N$ HSQC experiments optimized to retain full sensitivity. *J. Magn. Reson. 102*, 241−245.
(38) Wüthrich, K. (1986) *NMR of proteins and nucleic acids*, John Wiley & Sons, New York.
(39) Thomas, P. D., Basus, V. J., and James, T. (1991) Protein solution structure determination from two-dimensional nuclear Overhauser effect experiments: Effect of approximations on the accuracy of derived structures. *Proc. Natl. Acad. Sci. U.S.A. 88*, 1237−1241.
(40) Pronk, S., Szilard, P., Schulz, R., Larsson, P., Bjlkmar, P., Apostolov, R., Shirts, M. R., Smith, J. C., Kasson, P. M., Van der Spoel, D., and Lindahl, E. (2013) GROMACS: A high-throughput and highly parallel open source molecular simulation toolkit. *Bioinformatics 29*, 845−854.
(41) Jorgensen, W. L., and Severence, D. (1990) Aromatic-aromatic interactions: Free energy profiles for the benzene dimer in water, chloroform, and liquid benzene. *J. Am. Chem. Soc. 112*, 4768−4774.
(42) Berendsen, H. J. C., Postma, J., van Gunsteren, W. F., and Hermans, J. (1981) Interaction models for water in relation to protein hydration. *Nature 224*, 175−177.
(43) Berendsen, H., Postma, J., DiNola, A., and Haak, J. (1984) Molecular dynamics with coupling to an external water bath. *J. Chem. Phys. 81*, 3684−3690.
(44) Darden, T., York, D., and Pedersen, L. (1993) Particle mesh Ewald: An W log(N) method for Ewald sums in large systems. *J. Chem. Phys. 98*, 10089.
(45) Hess, B., Bekker, H. J. C., and Fraaije, J. G. E. M. (1997) LINCS: A linear constraint solver for molecular simulations. *J. Comput. Chem. 18*, 1463−1472.
(46) Hukushima, K., and Nemoto, K. (1996) Exchange Monte Carlo Method and Applicationto Spin Glass Simulations. *J. Phys. Soc. Jpn. 65*, 1604−1608.
(47) Okabe, T., Kawata, M., Okamoto, Y., and Mikami, M. (2001) Replica-exchange Monte Carlo method for the isobaric-isothermal ensemble. *Chem. Phys. Lett. 335*, 435−439.
(48) Seibert, M. M., Patriksson, A., Hess, B., and van der Spoel, D. (2005) Reproducible polypeptide folding and structure predition using molecular dynamics simulations. *J. Mol. Biol. 354*, 173−174.
(49) Patriksson, A., and van der Spoel, D. (2008) A temperature calculator for replica exchange molecular dynamics simulations. *Phys. Chem. Chem. Phys. 10*, 2073−2077.
(50) Szilágyi, L. (1995) Chemical shifts in proteins come of age. *Prog. Nucl. Magn. Reson. Spectrosc. 27*, 325−443.
(51) Szilágyi, L., and Jardetzky, O. (1989) α-Proton chemical shifts and secondary structure in proteins. *J. Magn. Reson. 83*, 441−449.
(52) Wishart, D. S., Sykes, B. D., and Richards, F. M. (1992) The chemical shift index: A fast and simple method for the assignment of protein secondary structure through NMR spectroscopy. *Biochemistry 31*, 1647−1651.
(53) Shen, Y., and Bax, A. (2007) Protein backbone chemical shifts predicted from searching a database for torsion angle and sequence homology. *J. Biomol. NMR 38*, 289−300.
(54) Pardi, A., Wagner, G., and Wüthrich, K. (1983) Protein conformation and proton nuclear-magnetic resonance chemical shifts. *Eur. J. Biochem. 137*, 445−454.
(55) Neal, S., Nip, A., Zhang, H., and Wishart, D. (2003) Rapid and accurate calculation of protein ^{1}H, ^{13}C and ^{15}N chemical shifts. *J. Biomol. NMR 26*, 215−240.
(56) Wang, Y., and Jardetzky, O. (2002) Investigation of the neighboring residue effects on protein chemical shifts. *J. Am. Chem. Soc. 124*, 14075−14084.
(57) Dyson, H. J., and Wright, P. E. (1994) Protein Structure Calculation Using NMR Restraints. In *Two-Dimensional NMR Spectroscopy Applications for Chemists and Biochemists*, 2nd ed., John Wiley & Sons, New York.
(58) Pardi, A., Billeter, M., and Wuthrich, K. (1984) Calibration of the angular dependence of the amide proton-C_a proton coupling constants $^{3}J_{NHa}$ in globular protein. Use of $^{3}J_{NHa}$ for identification of helical secondary structure. *J. Mol. Biol. 180*, 741−751.
(59) Van der Spoel, D. (1998) The solution conformations of aminoacids from molecular dynamics simulations of Gly-X-Gly peptides: Comparison with NMR parameters. *Biochem. Cell Biol. 76*, 164−170.
(60) Karplus, M. (1959) Contact electron-spin coupling of nuclear magnetic moments. *J. Chem. Phys. 30*, 11−15.
(61) Vuister, G. W., and Bax, A. (1993) Quantitative J correlation: A new approach for measuring homonuclear three-bond $J(H^{N}−H^{\alpha})$ coupling constants in ^{15}N-enriched proteins. *J. Am. Chem. Soc. 115*, 7772−7777.
(62) Gibbons, W. A., Beyer, C. F., Dadok, J., Sprecher, R. F., and Wyssbrod, H. R. (1975) Studies of individual amino acid residues of the decapeptide tyrocidine A by proton double-resonance difference spectroscopy in the correlation mode. *Biochemistry 14*, 420−429.
(63) Kuo, M. C., and Gibbons, W. A. (1980) Nuclear Overhauser effect and cross-relaxation rate determinations of dihedral and transannular interproton distances in the decapeptide tyrocidine A. *Biophys. J. 32*, 807−836.
(64) Pal, D., and Chakrabarti, P. (2002) On residues in the disallowed region of the ramachandran map. *Biopolymers 63*, 195−206.
(65) Mahalakshmi, R., and Balaram, P. (2007) The use of D-amino acids in peptide design. In *D-Amino Acids: A New Frontier in Amino Acid and Protein Research—Practical Methods and Protocols* (Konno, R., Bruckner, H., D'Aniello, A., Fisher, G., and Fujii, N., Eds.) 1st ed., pp 415−430, Nova Publishers.
(66) Jelokhani-Niaraki, M., Hodges, R. S., Meissner, J. E., Hassenstein, U. E., and Wheaton, L. (2008) Interaction of gramicidin S and its aromatic amino acid analog with phospholipid membranes. *Biophys. J. 95*, 3306−3321.
(67) Laiken, S., Printz, M., and Craig, L. C. (1969) Circular dichroism of the tyrocidines and gramicidin S-A. *J. Biol. Chem. 244*, 4454−4457.
(68) Lee, D. L., Powers, J. P. S., Pflegerl, K., Vasil, M. L., Hancock, R. E. W., and Hodges, R. S. (2004) Effects of single D-amino acid substitutions on disruption of β-sheet structure and hydrophobicity in cyclic 14-residue antimicrobial peptide analogs related to gramicidin S. *J. Pept. Res. 63*, 69−84.
(69) Krittanai, C., and Johnson, W. C. (1997) Correcting the circular dichroism spectra of peptides for contributions of absorbing side chains. *Anal. Biochem. 253*, 57−64.
(70) Daura, X., van Gunsteren, W. F., and Mark, A. E. (1999) Folding-unfolding thermodynamics of a β-heptapeptide from equilibrium simulations. *Proteins: Struct., Funct., Genet. 34*, 269−280.
(71) Hotchkiss, R. D. (1944) Gramicidin, Tyrocidine and Tyrothricin. *Adv. Enzymol. Relat. Areas Mol. Biol. 4*, 153−183.
(72) Stern, A., Gibbons, W. A., and Craig, L. C. (1968) A conformational analysis of gramicidin S-A by nuclear magnetic resonance. *Proc. Natl. Acad. Sci. U.S.A. 61*, 734−741.
(73) Rackovsky, S., and Scheraga, H. A. (1968) Intermolecular antiparallel β-sheet: Comparison of predicted and observed conformations of gramicidin S. *Proc. Natl. Acad. Sci. U.S.A. 77*, 6965−6967.
(74) Liquori, A., and De Santis, P. (1980) X-ray structure versus predicted conformation of gramicidin S. *Int. J. Biol. Macromol. 2*, 112−115.

(75) Izumiya, N., Kato, T., Aoyagi, H., Waki, M., and Kondo, M. (1979) *Synthetic Aspects of Biologically Active Cyclic Peptides-Gramicidin S and Tyrocidines*, John Wiley & Sons, New York
(76) Llamas-Saiz, A. L., Grotenbreg, G. M., Overhand, M., and van Raaij, M. J. (2007) Double-stranded helical twisted β-sheet channels in crystals of gramicidine S grown in the presence of trifluoroacetic and hydrochloric acids. *Acta Crystallogr. D63*, 401−407.
(77) Jang, H., Arce, F. T., Mustata, M., Ramachandran, S., Capone, R., Nussinov, R., and Lal, R. (2011) Antimicrobial protegrin-1 forms amyloid-like fibrils with rapid kinetics suggesting a fuctional link. *Biophys. J. 100*, 1775−1783.
(78) Kagan, B. L., Jang, H., Capone, R., Teran Arce, F., Ramachandran, S., Lal, R., and Nussinov, R. (2012) Antimicrobial properties of amyloid peptides. *Mol. Pharmaceutics 9*, 708−717.